Deep Learning in Lung and Colon Cancer classifications

Krishna Mridha
Computer *Engineering Marwadi University* Rajkot, India
krishna.mridha108735@marwadiuniversity.ac.in

MD. Iftekhar Islam
Department of Electrical and Electronic Engineering
American International University Bangladesh, Dhaka, Bangladesh

Shamin Ashfaq
Department of Computer Science and Engineering
Southeast University
shamin.asfaq@gmail.com

Masrur Ahsan Priyok
Software Engineering
Tianjin University, China
masrurahsan8@gmail.com

Dipayan Barua
Informaation Technology
Marwadi Univeristy, Rajkot, India
Dipayan.barua108033@marwadiuniversity.ac.in

2022 International Conference on Advances in Computing, Communication and Materials (ICACCM) | 978-1-6654-7439-9/22/$31.00 ©2022 IEEE | DOI: 10.1109/ICACCM56405.2022.10009311

***Abstract*— The past few decades have seen revolutionary advancements in the field of Healthcare and Medicine. During this period, the underlying reasons for many fatal diseases have been unveiled, novel diagnosis techniques were invented, and medical solutions were developed. Instead of these breakthroughs, we are still vulnerable and haunted by certain diseases like cancer. Globally, cancer is the second most common cause of mortality which accounts for the death of one in every six affected individuals. Among many other types, the colon and lung are the most prevailing and life-threatening ones. Only these two variants are responsible for 25% of all cancer cases around the world. However, early lung and colon cancer detection can significantly enhance the possibility of survival. Currently, Deep Learning (DL) has facilitated the automated identification of cancer cells which is allowing us to assess more patients in a minimum time and without the help of a medical professional. The study has put forward a DL framework to classify and differentiate five types of colon and lung cancer cells. Digital Image processing (DIP) and Deep Learning (DL) algorithms are used to process and evaluate histopathological images of cancer cells. The proposed framework has obtained a maximum testing accuracy of 98.3% in identifying and classifying cancer cells. By employing the proposed model in practice, medical experts will be able to integrate an accurate and automated system for diagnosing different forms of colon and lung cancers.**

Keywords—artificial intelligence, deep learning, image processing, lung cancer, colon cancer, histopathological image.

I. INTRODUCTION

Worldwide, lung and colon cancer is the most common reason of mortality for both men and women [7]. Primarily lung cancers can be categorized into two main types: non-small cell lung cancer and small cell lung cancer. With the current advancements in radiation therapy and chemotherapy [8], non-small cell lung cancer can be further categorized into squamous cell carcinoma, adenocarcinoma, and large cell carcinoma [9]. Due to their morphological characteristics, it is often very difficult to accurately define squamous cell carcinoma and adenocarcinoma. Immunohistochemical evaluation is proven to be efficient in differentiating these cancer cells. Additionally, in precisely defining small cell carcinoma, cyst diagnosis is proving to be advantageous over the histological specimen. To accurately define the different types of lung cancer cells, it is required to combine both the cytological and histopathological diagnoses as cancer cells contain different varieties of morphologies. Artificial intelligence (AI) guided diagnosis can be an effective solution in avoiding the misclassification of cancer cells. Due to its severe types, large cell carcinoma is the easiest to identify among the four main types of carcinomas. For this, the study has primarily concentrated to classify the other three main types- squamous cell carcinoma, adenocarcinoma, and large cell carcinoma to reduce the possibility of occurring misclassification.

On the other hand, to accurately identify the types of colon cancer cells, clinicians are dependent on several intricate diagnosis processes including ultrasound, CT scan, and a few histological evaluations [10]. However, predicting the presence of lymph node metastasis (LNM), a diagnosis of determining the severity of colon cancer, in colon cells is proving to be insufficient depending on these qualitative assessments of pathological features [11]. In histopathological examinations, AI-guided image analysis has been demonstrated to provide effective, accurate, and reliable quantitative extraction of features as well as decision-making assistance to guarantee diagnostic precision [12-13].

Currently, a doctor must go through multiple procedures, confer with specialists in lung and colon, and get second views before they can make a final decision on lung or colon cancer. In our project, the user will get a complete diagnosis, including the cell type, malignant state, and kind of malignancy, if relevant, by inputting a histopathological image of the colon or lung cancer cells into the model. By automating intermediary processes to produce a single comprehensive output diagnosis, ML speeds the process. Users do not necessarily need to be medical professionals; they could be assistants who relay the output to the specialist physician for evaluation. Thus, for doctors, our proposed framework serves as a "second opinion."

Table 1: Traditional System Vs. ML system

Medical Professional follows the below steps using ML	Medical professionals follow the below steps without using ML
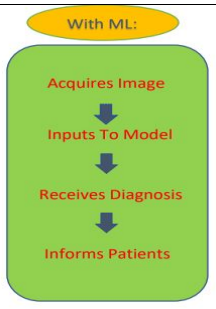	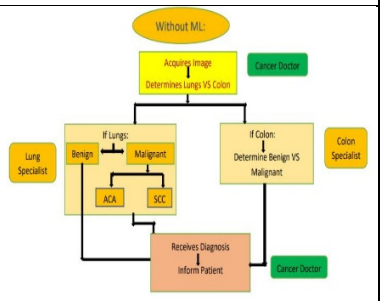

As there remains a wealth of datasets on which to examine and train our algorithm, we decided to categorize colon and lung tissues. A classifier able to categorize photos by organ can assist in situations where doctors are not the ones to collect images from a patient and prevent misunderstandings. Additionally, a batch of photos (perhaps each from a different patient) can be uploaded by users without having to manually arrange them or memorize their organ kinds. Sometimes both organs can be affected by adenocarcinoma which complicates the event. We intend to reduce situations in which cancer is accurately diagnosed but the respective organ is misidentified by implementing an organ differentiation phase.

II. Literature Review

ML is a developing technology that is showing increasing promise for use in the treatment of cancer. Algorithms are being designed to identify the most prevalent forms of cancer affecting the breast, bone, lung, skin, brain, and prostate [1,2].

In detecting cancer, a recent initiative has received noteworthy praise for its exceptional effectiveness [3]. Imperial College London in cooperation with Google Health took an initiative to leverage technology that will be able to enhance the screening procedures for breast cancer [3]. A sample set of 29,000 mammograms was used to construct the algorithm, which was then evaluated against the expertise of radiologists [3]. The algorithm's efficacy was shown to be superior to that of a two-person team when tested against one radiologist [3].

This algorithm's advantages are quite alluring because they provide time savings and can assist medical organizations by minimizing the dependency on radiologists [3]. Theoretically, this algorithm ought to be able to supplement a single radiologist's judgment to produce the best results [3].

Selvanambi et al [14] developed a method based on the Glowworm Swarm Optimization (GSO) for identifying lung cancer by using image datasets from many sources. A recurrent Neural Network (RNN) was chosen for the study and the model was able to obtain 98% precision. De Carvalho Filho et al. [15] developed an identification framework for lung cancer based on the CNN platform and experimented on 50,000 CT scan images.

An RF-based classification approach was proposed by Babu et al. [16] to anticipate the presence of colon cancer by assessing histopathological images of cancer cells. In the study, RGB images were taken to the HSV plane and wavelet decomposition was performed to extract features. They were able to obtain an accuracy of 85% by changing the magnification level of images.

By using colonoscopy images, Urban et al. [17] developed a method to identify polyps. The model obtained an accuracy of 96%. 8641 colonoscopy images were hand labeled by the researchers which they gathered from 2000 patients. A dataset was prepared by them to train a CNN model. Akbari et al [18] identified colorectal cancer by developing a CNN-based classifier and using colonoscopy videos. The model took into account the binarized weight network and obtain an accuracy of 90% in classifying colon cancer.

A comparable objective of our effort is to use AI to determine whether cancer is present in scans. The accomplishment of this breast cancer algorithm demonstrates that ML can finish this assignment with outstanding outcomes.

III. Methodology

This section has discussed the suggested methodology. This research study has used four Convolutional Neural Network (CNN) models getting a reference from GitHub [6]. Preprocessing the dataset's photos is strongly encouraged before doing any work. Preprocessed data will therefore aid in increased accuracy. This dataset has been normalized and preprocessed before being fed into the proposed architecture.

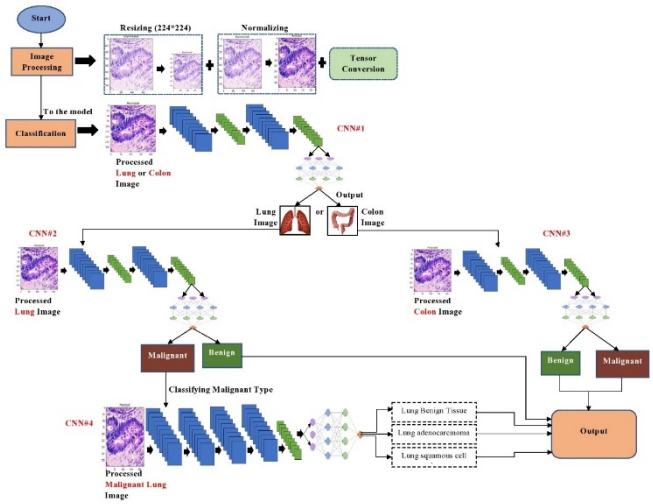

Figure 1: Research Illustration

Figure 1 describes the illustration of our work. The prosed architecture has four Convolutional Neural Network (CNN) models namely CNN #1, CNN #2, CNN #3, and CNN #4. All of these models solve only binary classification problems which means the models receive images as inputs and then it will provide binary class output. Each CNN models have a separate classification problem. The model starts from the Lung and Colon types of cancer classification and with its subtype cancer name.

3.1. Data Extraction/ Importing Data and Setup: The dataset is collected from Kaggle which is publicly available. The name of this dataset is "Lung and Colon Cancer Histopathological Images". The dataset contains histopathological images of five different types of cancer instance Lung adenocarcinoma, Lung benign tissue, Lung squamous cell carcinoma, Colon benign tissue, and Colon malignant. The number of images per class is 2500. So, the dataset has a total of 12, of 500.

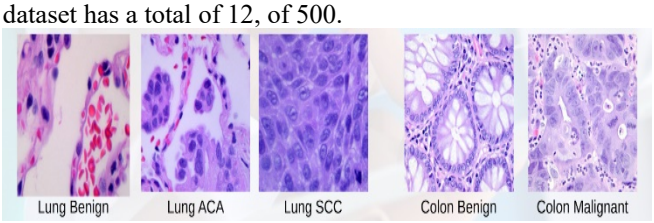

Figure 2: Samples image for perc class

Figure 1 is representing the images per class extracted from the dataset. There are three types of cancer for Lung data, for instance, Lung Benign, Lung ACA, and Lung SCC, for the Colon, there are two different types of cancer cells: Malignant and Malignant.

3.2. Exploratory Data Analysis (EDA): After importing the dataset or extracting the data, the next step is to analyze the data by using some advanced techniques that can help to understand the depth of the data. Here in this research, three steps have been taken for EDA. The Steps are mentioned below as:

3.2.1. Analysis of the Dataset: The dataset has five types of cancer that are equally distributed. Moreover, the dataset has a very less amount of observation in terms of class. Because the number of classes is five but the images are 12, 500. It is observed that the dataset is not too large, so it is possible to get very poor performance of the model output.

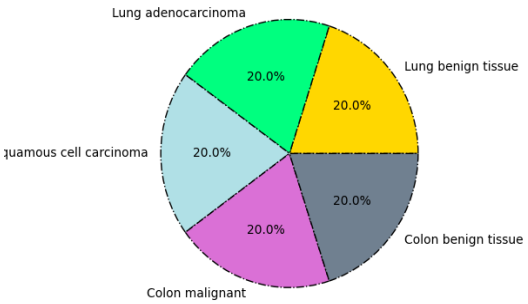

Figure 3: Percentage of Images in each Target Class

Figure 2. is representative of the distribution of each class occurrence. This pie chart shows that the dataset is equally distributed but in terms of performance, it is possible to get very low accuracy because the number of observations of each class is only 2500.

3.2.2. Image pre-processing: After collecting the dataset, the next step is to pre-process the data because the model does not perform up to mark with row data. So, Image pre-processing is one of the major tasks before training any deep learning network. The 25,000 total photos in this dataset were pre-augmented from 250 images of each class to 5,000 images of each class [4]. To maintain consistency and lighten the load on our proposed model, the pixel intensity of the photos is normalized to the range of [0,1]. Finally, tensors were created from photos.

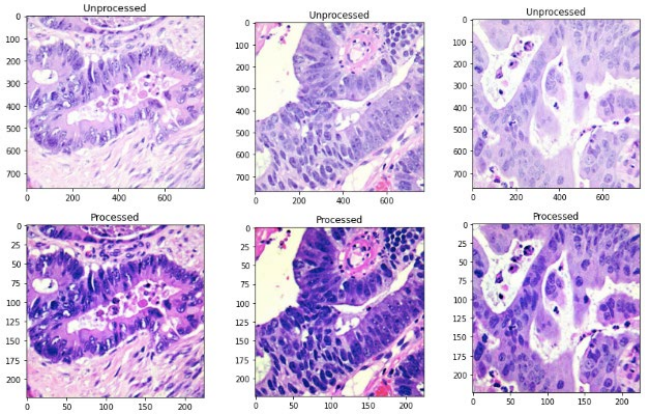

Figure 4: Data Visualization of Unprocessed vs proceed data

3.3. Data Augmentation: Data Augmentation is one of the best ways to overcome the small dataset problem. This dataset has only 12, 500 images before augmentation. By using data generator methods from TensorFlow, the images are increased to 5,000 for each class. That means the total number of images is 25,000 a very healthy number of observations. Even though, there are lots of operation available for data augmentation, some of them are using for this dataset for instance rotation_range = 40, shear_range = 0.2, zoom_range = 0.2, horizontal_flip = True, brightness_range = (0.5, 1.5).

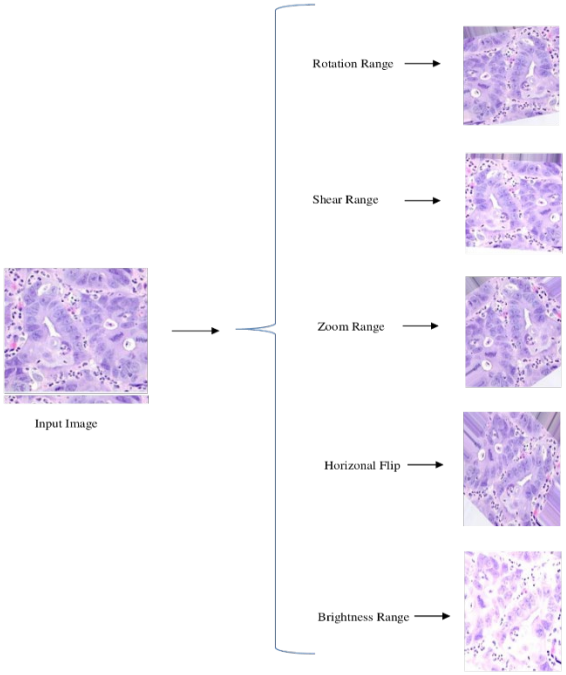

Figure 5: Data Augmentation of an Input Image by using five operations.

3.4 Train, Test, and Validation: Since the dataset we used had undergone extensive preprocessing, dividing and sorting the data were our primary processing tasks. Since our classifier consists of four connected CNNs, it was required to make sure that:

- For the classification task, each CNN consists suitable dataset.
- The dataset for each CNN was balanced.
- All CNNs are trained with a portion of the same training set.
- A segment of the same testing set that NONE of the CNNs had previously seen was used to test each CNN separately.
- A novel set that no individual CNN had ever seen in training, validation, or individual testing was used to fully test the entire model of linked CNNs.

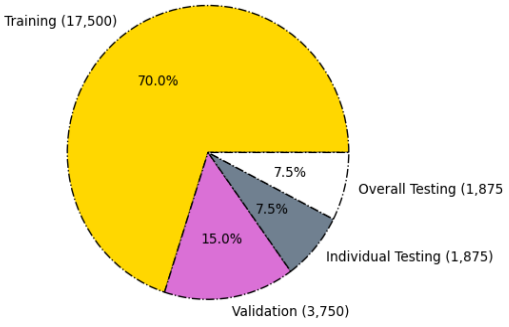

Figure 6: Percentage of Trian, Test, and Validation data set

To do this, the dataset was divided into four sets with the following ratios: training, validation, individual testing, and overall testing with ratios respectively 70:15:7.5:7.5. From them, we developed unique model datasets, as displayed below:

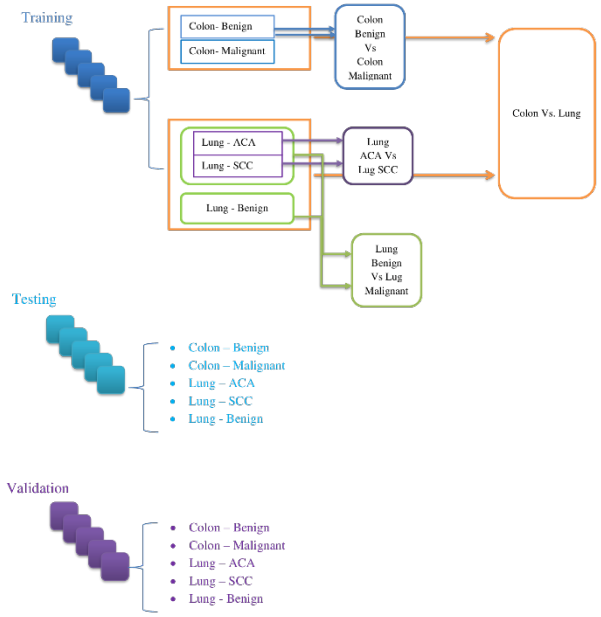

Figure 7: Training, Testing, and Validation Steps

3.5. Model Design: In the architecture, there are four distinct binary CNNs. Each CNN receives a single 224x224 square picture that has been previously processed, and it outputs either a one or a zero depending on the categorization that the framework determines. The first CNN makes a distinction between the colon and thoracic scans. The image is forwarded to CNN #2, which can discriminate the cancerous and benign lung tissues if it is determined to be a lung scan. If a colon scan is detected, the image is forwarded to CNN #3, which can tell the difference between benign and cancerous colon cells. Adenocarcinoma or squamous cell carcinoma is the fourth CNN used to categorize the kind of lung cancer.

Convolutional Neural Network – CNN#1 (Lung Vs. Colon):

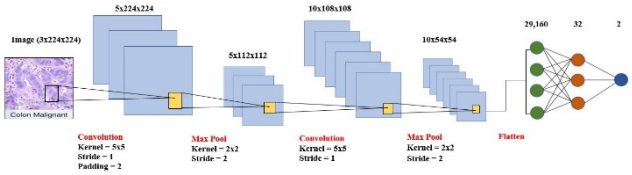

Figure 8: CNN#1 for Lung Vs. Colon Cancer

Figure 8 is called CNN#1 which is a binary classification algorithm for Lung vs. Colon cancer. The model consists of 2 convolutional layers with kernel 5x5, padding 2, and stride 1. The reason behind selecting padding size 2 is not to lose any important information after the first ConvNet whereas the second ConvNet does not has padding. Additionally, there are 2 max-pooling layers with kernel 2x2 and stride 2 used and after getting an output of 29,160 from the 2nd max pooling layer it passes through one Fully Connected (FC) which has 32 neurons. Finally, the output of the vector is the size of 29,160x32 and passed to the classifier for prediction by using the sigmoid function.

Convolutional Neural Network – CNN#2 (Lung Benign Vs. Lung Malignant):

Figure 9 is called CNN#2 which is a binary classification algorithm of Lung Benign vs. Lung Malignant. The model consists of 1 convolutional layer with kernel 5x5, padding 2, and stride 1. Additionally, there are 2 conjugative pooling layers.

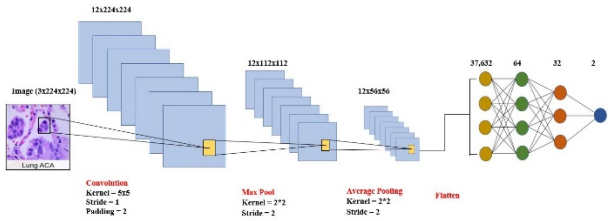

Figure 9: CNN#2 Lung Benign Vs. Lung Malignant

The first one is the max pooling layer and the second one is the average pooling layer with kernel 2x2 and strides 2 used after getting output 37632 from the 2nd pooling layer passing through two Fully Connected (FC) which have 64 and 32 neurons. Finally, the output of the vector is the size of 37632x64x32 and passed to the classifier for prediction by using the sigmoid function.

Convolutional Neural Network – CNN#3 (Colon Benign Vs. Colon Malignant):

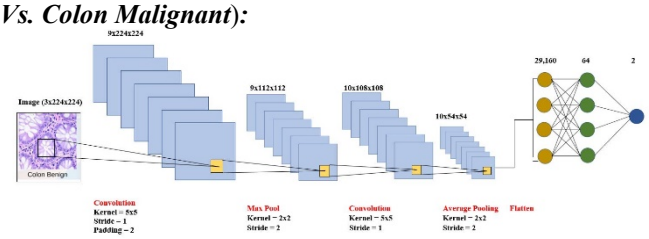

Figure 10: CNN#3 for Colon Benign Vs. Colon Malignant

Figure 10 is called CNN#3 which is a binary classification algorithm of Colon Benign vs. Colon Malignant. The model consists of 2 convolutional layers with kernel 5x5, padding 2, and stride 1. Additionally, there are 2 max-pooling layers with kernel 2x2 and stride 2 used. The first one is the max pooling layer and the second one is the average pooling layer with kernel 2x2 and stride 2 used after getting an output of 29,160 from the 2nd pooling layer passing through one Fully Connected (FC) which has 64 neurons. Finally, the output of the vector is the size of 29,160x64 and passed to the classifier for prediction by using the sigmoid function.

Table 2: Table 1: Each Convolutional Network with Hypermeter

Model Name	Batch Size	Learning Rate	# Of Epochs	# Of Convolution Layers	# Of Pooling Layers	# Of Fully Connected Layers
CNN 1: Lung Vs. Colon	240	0.01	14	2	2	1
CNN 2: Lung Benign vs. Malignant	135	0.01	9	1	2	2
CNN 3: Colon Benign vs. Malignant	240	0.01	14	2	2	1
CNN 4: Lung SCC vs. ACA	120	0.01	13	2	2	1

Convolutional Neural Network – CNN#4 (Lung ACA Vs. Lung SCC):

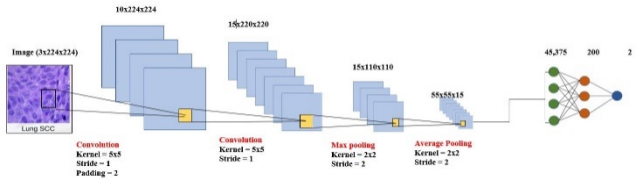

Figure 11: CNN#4 for Lung ACA Vs. Lung SCC

Figure 11 is called CNN#4 which is a binary classification algorithm of Lung ACA vs. Lung SCC which are two dangerous subtypes of Lung cancer. The model consists of 2 conjugative convolutional layers with kernel 5x5, padding 2 (only for ConvNet), and stride 1. Additionally, there are also 2 conjugative pooling layers with kernel 2x2 and stride 2 used. The first one is the max pooling layer and the second one is the average pooling layer with kernel 2x2 and stride 2 used after getting an output of 45,375 from the 2nd pooling layer passing through one Fully Connected (FC) which has 200 neurons. Finally, the output of the vector is the size of 45,375x 200 and passed to the classifier for prediction by using the sigmoid function.

IV. Results and Discussion

In the architecture, there are four distinct binary CNNs. Each CNN receives a single 224x224 square picture that has been previously processed, and it outputs either a one or a zero depending on the categorization that the framework determines. The first CNN makes a distinction between the colon and thoracic scans. The image is forwarded to CNN #2, which can discriminate the cancerous and benign lung tissues if it is determined to be a lung scan. If a colon scan is detected, the image is forwarded to CNN #3, which can tell the difference between benign and cancerous colon cells. Adenocarcinoma or squamous cell carcinoma is the fourth CNN used to categorize the kind of lung cancer. The invariance features of the CNN architecture were the deciding factors [5]. In this context, a framework is required which will be able to find more intricate patterns that may be present since there is a lot of variation across photos, including variations in cell size orientation, and placement [5].

Table 2 is representing the parameters of all of the models where all of the CNN models' structures are different. The models are optimized with the hypermeter's values. The Learning rate is the same for each CNN model.

The numbers of epochs, ConvNet, pooling layers, and FC layers all are hypermeter values.

Table 3: Results from the Confusion Matrix

	Colon Benign	Colon Malignant	Lung ACA	Lung Benign	Lung SCC
Colon ACA	361	72	0	1	0
Colon Malignant	6	300	0	0	0
Lung ACA	4	3	352	0	49
Lung Benign	4	0	5	368	1
Lung SCC	0	0	18	6	325
Accuracy	**361/375 = 96%**	**300/375 = 80%**	**352/375 =94%**	**368/375 = 98%**	**325/375 = 87%**

Table 2 represents the output of models for overall testing images. We have chosen 7.5% (1875) images from 25,000 as our overall testing images. So, per class testing image will be 1875/5 = 375. The best class accuracy got from Lung Benign is about 98% and the overall accuracy will be 91% which belongs to a very good performance category. Below, is the error table shows for each class.

Table 4: Error Analysis according to Table 2

False Positive (Classify non-cancerous as cancer	1.6% (as Malignant)			1.6% (as Lung ACA)	
False Negative (Classify cancerous as non-cancer)		19.2 % (as Colon Benign)	1.3 % (as Lung Benign)		0.26% (as Benign)
Incorrect Cancer type (Classify ACA as SCC and vice-versa)			4.8% (as Lung SCC)		13.1% (as ACA)
Wrong Organ (Classify Colon as Lung and vice-versa)	2.1% (as Lung)	0.8 % (as Lung)		0.26% (as Colon)	
Total Error	3.7%	20%	6%	2%	13%

Table 3 represents the error values of the particular class. The errors are measured by four metrics for instance False Negative, False positive, Incorrect cancer type, and the wrong organ classification. The table describes that the False-negative values for Colon malignant showing more error (19%) marked as red-colored because its' original output is cancerous but it is predicted as non-cancerous. Other normal errors are marked as blue-colored. The more versatile convolutional neural networks (CNN #1 and CNN #2) have extremely high accuracy. CNN's #3 and #4 on the peripheral made up the majority of the errors. This made sure that error propagation was kept to a minimum.

Table 5: Training, Validation, & Testing Accuracies for Each Convolutional Neural Network

	Training Accuracy	Validation Accuracy	Testing Accuracy
CNN 1: Lung vs. Colon	98.99%	97.99%	97.99%
CNN 2: Lung Benign vs. Malignant	98.79%	98.1%	98.3%
CNN 3: Colon Benign vs. Malignant	99%	94.5%	96.1%
CNN 4: Lung SCC vs. ACA	96.0%	90.1%	89.5%

False-negative rates were particularly low for the colon and lung, suggesting that the framework would infrequently disregard a malignant scan. This is crucial because false negative results may lead a patient to seek care at a later time when cancer will be more deleterious. This crucial flaw is absent from the proposed model.

One drawback is that colon scans have the propensity to produce false positive results. The model regularly misidentified cancer in healthy colon scans. A healthy patient can end up having an extra scan or biopsy as a result, which could be costly or uncomfortable. Even though this is less dangerous than falsely classifying something as negative, it could nonetheless be harmful.

Table 6: Error/Loss Training Curves for Each Convolutional Neural Network

V. Conclusion

The two most common malignancies in the world are lung and colon. The therapy results and survival rates of certain cancer can be considerably increased with an early and accurate diagnosis. Accurate and effective lung and colon cancer detection was the aim of this study. It is crucial to evaluate the benefits of an algorithm using four binary neural networks rather than a single conventional multi-class CNN given our novel approach to the issue. The multi-class classifier had several drawbacks that we identified, including decreased accuracy (having initially only achieved 65%), memory and time-intensive training (given that it would deal with much more images segmented into 5 classes), and other issues. With 4 distinct binary networks, the algorithm may be precisely tuned at each step. Additionally, the misdiagnosis of cancers of comparable types is greatly decreased by using a high-precision model that differentiates organs as the initial step (Lung ACA vs. Colon ACA). We have become aware of the importance of having preprocessed data as a result of creating this repository. Though for testing and developing a model, a prepared dataset might be ideal, the same model may not function as well on data that has undergone a distinct processing method (arranged with different dyes, etc.). Additionally, aggregate precision results are often misleading, and false negative/positive scores are a more accurate way to pinpoint a model's flaws. The fact that a distinct binary framework performed better than a multi-class classifier in our situation shows that a conventional approach to an issue is not necessarily the best one. The accuracy of the proposed methodology for detecting lung and colon cancer has not only surpassed that of cutting-edge methods but has also saved time and money. We think that the effective diagnosis of other diseases can also be attributed to our proposed methodology.

References

[1] Capper, D., Jones, D.T., Sill, M., Hovestadt, V., Schrimpf, D., Sturm, D., Koelsche, C., Sahm, F., Chavez, L., Reuss, D.E. and Kratz, A., 2018. DNA methylation-based classification of central nervous system tumors. Nature, 555(7697), pp.469-474.

[2] Cao, R., Bajgiran, A.M., Mirak, S.A., Shakeri, S., Zhong, X., Enzmann, D., Raman, S. and Sung, K., 2019. Joint prostate cancer detection and Gleason score prediction in mp-MRI via FocalNet. IEEE transactions on medical imaging, 38(11), pp.2496-2506.

[3] Yala, A., Lehman, C., Schuster, T., Portnoi, T. and Barzilay, R., 2019. A deep learning mammography-based model for improved breast cancer risk prediction. Radiology, 292(1), pp.60-66.

[4] Ardila, D., Kiraly, A.P., Bharadwaj, S., Choi, B., Reicher, J.J., Peng, L., Tse, D., Etemadi, M., Ye, W., Corrado, G. and Naidich, D.P., 2019. End-to-end lung cancer screening with three-dimensional deep learning on low-dose chest computed tomography. Nature medicine, 25(6), pp.954-961.

[5] S. Kumar, Anna, Justing T. Harrison, AICancer repository in Github, https://github.com/justin13601/AICancer

[6] American Cancer Society, Cancer Facts and Figures 2015.

[7] P. Baas et al., "Concurrent chemotherapy (carboplatin, paclitaxel, etoposide) and involved-field radiotherapy in limited stage small cell lung cancer: a Dutch multicenter phase II study", British Journal of Cancer, vol. 94, no. 5, pp. 625-630, 2006. Available: 10.1038/SJ.bjc.6602979 [Accessed 12 August 2022].

[8] W. Travis et al., "The 2015 World Health Organization Classification of Lung Tumors", Journal of Thoracic Oncology, vol. 10, no. 9, pp. 1243-1260, 2015. Available: 10.1097/jto.0000000000000630 [Accessed 12 August 2022].

[9] T. Pelkey, H. Frierson, and D. Bruns, "Molecular and immunological detection of circulating tumor cells and micrometastases from solid tumors", Clinical Chemistry, vol. 42, no. 9, pp. 1369-1381, 1996. Available: 10.1093/clinchem/42.9.1369 [Accessed 12 August 2022].

[10] D. Weaver, "Sentinel Lymph Nodes and Breast Carcinoma", The American Journal of Surgical Pathology, vol. 27, no. 6, pp. 842-845, 2003. Available: 10.1097/00000478-200306000-00018 [Accessed 12 August 2022].

[11] J. Hipp et al., "Computer-aided diagnostic tools aim to empower rather than replace pathologists: Lessons learned from computational chess", Journal of Pathology Informatics, vol. 2, no. 1, p. 25, 2011. Available: 10.4103/2153-3539.82050 [Accessed 12 August 2022].

[12] P. Hamilton et al., "Digital pathology and image analysis in tissue biomarker research", Methods, vol. 70, no. 1, pp. 59-73, 2014. Available: 10.1016/j.ymeth.2014.06.015 [Accessed 12 August 2022].

[13] R. Selvanambi, J. Natarajan, M. Karuppiah, S. Islam, M. Hassan, and G. Fortino, "Lung cancer prediction using higher-order recurrent neural network based on glowworm swarm optimization", Neural Computing and Applications, vol. 32, no. 9, pp. 4373-4386, 2018. Available: 10.1007/s00521-018-3824-3 [Accessed 12 August 2022].

[14] A. de Carvalho Filho, A. Silva, A. de Paiva, R. Nunes, and M. Gattass, "Classification of patterns of benignity and malignancy based on CT using topology-based phylogenetic diversity index and convolutional neural network", Pattern Recognition, vol. 81, pp. 200-212, 2018. Available: 10.1016/j.patcog.2018.03.032 [Accessed 12 August 2022].

[15] T. Babu, D. Gupta, T. Singh, and S. Hameed, "Colon Cancer Prediction On Different Magnified Colon Biopsy Images," 2018 Tenth International Conference on Advanced Computing (ICoAC), 2018, pp. 277-280, DOI: 10.1109/ICoAC44903.2018.8939067.

[16] G. Urban et al., "Deep Learning Localizes and Identifies Polyps in Real Time With 96% Accuracy in Screening Colonoscopy", Gastroenterology, vol. 155, no. 4, pp. 1069-1078.e8, 2018. Available: 10.1053/j.gastro.2018.06.037.

[18] M. Akbari et al., "Classification of Informative Frames in Colonoscopy Videos Using Convolutional Neural Networks with Binarized Weights," 2018 40th Annual International Conference of the IEEE Engineering in Medicine and Biology Society (EMBC), 2018, pp. 65-68, DOI: 10.1109/EMBC.2018.8512226.